Mechanistic Aspects of the DNA Junction-Resolving Enzyme T7 Endonuclease I[†]

Jia Liu, Anne-Cécile Déclais, and David M. J. Lilley*

Cancer Research UK Nucleic Acid Structure Research Group, MSI/WTB Complex, The University of Dundee, Dundee DD1 5EH, U.K.

Received November 14, 2005; Revised Manuscript Received January 18, 2006

ABSTRACT: The chemical mechanism of phosphodiester bond hydrolysis catalyzed by a junction-resolving enzyme has been investigated. Endonuclease I of phage T7 is a member of the nuclease superfamily of proteins that include many restriction enzymes, and the structure of the active site is very similar to that of *Bgl*I in particular. It contains three acidic amino acids that coordinate two divalent metal ions. Using mass spectrometry we have shown that endonuclease I catalyzes the breakage of the P−O3′ bond, in common with restriction enzymes. We have found that the pH dependence of the hydrolysis reaction is log-linear, with a gradient of 0.9. Substitution of the scissile phosphate by an electrically neutral methylphosphonate significantly impairs the rate of bond cleavage. However, the introduction of chirally pure methylphosphonate groups shows that the effect of substitution of the *proS* oxygen atom is much greater than that for the *proR*. This is consistent with our current model of the structure of the DNA bound in the active site of endonuclease I, where the *proS* oxygen atom is coordinated directly to both metal ions as it is in *Bgl*I. The activity is also very sensitive to repositioning of the carboxylate groups of Asp 55 and Glu 65 in the active site, although some restoration of activity in endonuclease I E65D was observed in the presence of Mn^{2+} ions. A mechanism of hydrolysis consistent with all of these data is proposed.

Junction-resolving enzymes are nucleases that are selective for the structure of four-way DNA junctions. They catalyze the cleavage of phosphodiester linkages in the junction. However, there has been very little investigation of the chemical mechanism of these enzymes. In general, the junction-resolving enzymes catalyze the metal ion-dependent hydrolysis of two specific phosphodiester linkages in the junction (*1*). Coordinated pairwise cleavages on opposing strands (*2*, *3*) lead to the resolution of the junction into two nicked duplex species.

Junction-resolving enzymes have been isolated from a wide variety of sources, including bacteria (*4*, *5*) and their phages (*6*, *7*), yeast (*8*−*10*), and archaea (*11*, *12*). There is also good evidence for the existence of similar activities in mammals (*13*) and their viruses (*14*). Phylogenetic analysis of these enzymes indicates that the majority fall into one of two superfamilies (*15*, *16*). RuvC of *Escherichia coli* and Cce1 of *Saccharomyces cerevisiae* are classified with the integrase group that includes RNase H, while T7 endonuclease I and Hjc of *Sulfolobus solfataricus* fall into the family that includes the restriction enzymes and λ-endonuclease. Crystal structures of junction-resolving enzymes (*17*−*22*) reveal a variety of overall folds, but in general the active sites contain acidic side chains that can bind metal ions via their carboxylate groups. It is therefore probable that these enzymes are derived from an ancestral metal ion-binding protein and that hydrolysis is achieved by nucleophilic attack of a water molecule coordinated directly to a metal ion.

Endonuclease I is a basic 149 amino acid protein encoded by gene 3 of phage T7 (*23*−*25*) that is required for the resolution of branched DNA replication intermediates (*26*−*28*). We have solved the crystal structure of the enzyme with (*19*) and without (*29*) an active site mutation. The active site of endonuclease I conforms to the restriction enzyme consensus (*30*), i.e., (D/E20)...P54D55...(D/E65)XK67 (the residue numbers refer to endonuclease I), and the α and β carbon atoms of the four critical side chains (E20, D55, E65, and K67) plus the conserved proline (P54) can be superimposed with the structure of the corresponding residues of the restriction enzyme *Bgl*I (*31*) with an rmsd of 0.49 Å. Similar catalytic motifs also exist in λ-exonuclease (*32*), MutH (*33*), and TnsA (*34*), as well as the archaeal junction-resolving enzymes (*20*, *22*). Two Ca^{2+} ions were observed coordinated in the active site of *Bgl*I with a bound DNA fragment in the crystal structure (*31*), and we have found two Mn^{2+} ions in equivalent positions in the crystal structure of wild-type sequence endonuclease I in the absence of DNA (*29*). Binding of two metal ions to the protein was also indicated by isothermal titration calorimetry (*29*), and Fe(II)-mediated cleavage of DNA indicated a very similar location of metal ions in the complex (*35*). This suggests a common mechanism of DNA cleavage, requiring divalent metal ions coordinated by carboxylate groups (*36*).

In the present study we have investigated the catalytic mechanism of endonuclease I in greater detail. We have determined the direction of nucleophilic attack, and the pH dependence of the reaction is consistent with a metal-bound hydroxide ion acting as the active nucleophile. In addition, we have determined the relative importance of the two nonbridging oxygen atoms of the scissile phosphate by means

[†] This work was financially supported by Cancer Research U.K.

* To whom correspondence should be addressed. Tel: (+44)-1382-344243. Fax: (+44)-1382-345893. E-mail: dmjlilley@dundee.ac.uk.

10.1021/bi0523254 CCC: $33.50
Published on Web 03/03/2006

of stereospecific methylphosphonate substitution. All of the results are consistent with a proposed reaction mechanism based on comparisons with restriction enzymes.

MATERIALS AND METHODS

Expression and Purification of T7 Endonuclease I. Wild-type and mutant endonucleases I were expressed and purified using the same method as described previously (*19, 29*). The N-terminal decahistidine affinity tag was cleaved off using a mild tryptic digestion, and the digest was applied to an HS ion-exchange column (PerSeptive Biosystems). Protein concentrations were measured spectrophotometrically, using an absorption coefficient of 49500 M^{-1} cm^{-1} at 280 nm for a dimer. All protein concentrations cited in the text refer to dimers.

Site-Directed Mutagenesis of Endonuclease I. Site-directed mutagenesis using the QuickChange procedure from Stratagene was performed on the gene for endonuclease I in the expression vector. Two complementary mutagenic oligonucleotides were annealed to the double-stranded plasmid, which was then resynthesized with *Pfu* polymerase (Strategene) using PCR. Replicated mutated plasmid was incubated with the methylation-sensitive restriction enzyme *Dpn*I to digest the parental DNA plasmid. The mutant plasmid was transformed into *E. coli*, and plasmid DNA was prepared and sequenced.

Construction of DNA Junctions. Oligodeoxyribonucleotides were synthesized using standard phosphoramidite chemistry (*37*) implemented on an Applied Biosystems 394 synthesizer. Methylphosphonamidites (Glen Research) were incorporated using an extended coupling time. Unmodified oligonucleotides were deprotected with ammonia at 55 °C for 16 h. Methylphosphonate-modified oligonucleotides were deprotected in an acetonitrile/ethanol/ammonium hydroxide mixture (45:45:10) at room temperature for 30 min. An equal volume of ethylenediamine was then added, and the mixture was left for a further 6 h. The supernatant was collected, and the support was washed twice with 1 mL of acetonitrile/water (1:1). The pH of the combined supernatants was adjusted to 7 with 6 M hydrochloric acid in acetonitrile/water (1:9). The oligonucleotides were then desalted using Poly-Pak cartridges (Glen Research). All oligonucleotides were purified by electrophoresis in polyacrylamide gels containing 7 M urea. DNA was recovered from gel fragments by electroelution followed by ethanol precipitation. Where required, oligonucleotides were radioactively 5′-^{32}P-labeled using T4 polynucleotide kinase and [γ-^{32}P]ATP (Amersham).

Construction of Junction S. Junction 3 with extended B and X arms was constructed by hybridizing the four oligonucleotides (all sequences written 5′ to 3′):

b strand, CGCAAGCGACAGGAACCTCGAGGGATCCGTCCTAGCAAGGGGCTGCTACCGGAA; h strand, TTCCGGTAGCAGCCmpTGAGCGGTGGTTGA; r strand, TCAACCACCGCTCAACTCAACTGCAGTCTAGACTCGAGGTTCCTGTCGCTTGCG; x strand, CGCAAGCGACAGGAACCTCGAGTCTAGACTGCAGTTGAGTCCTTGCTAGGACGGATCCCTCGAGGTTCCTGTCGCTTGCG. The h strand contained a methylphosphonate linkage at the center, indicated by mp. Two forms of the junction containing the alternative diastereomers of the methylphosphonate were separated by electrophoresis in 8% polyacrylamide gels (29:1, acrylamide:bisacrylamide) in 90 mM Tris−borate (pH 8.3) and 200 μM $MgCl_2$ for 25 h at 120 V at 20 °C, with recirculation of the buffer at >1 L h^{-1}. From our previous studies it is known that the slow-migrating species contains the S_p diastereomer, while the fast-migrating species contains the R_p diastereomer (*38*). Junctions were visualized by UV shadowing and recovered by electroelution followed by ethanol precipitation. The chirally pure h strand species were purified from the remaining strands by gel electrophoresis in a denaturing polyacrylamide gel containing 7 M urea, followed by electroelution from the excised gel fragments containing the 28 nt species. These (and the racemic form of the strand) were then separately hybridized to three new strands, i.e., b′ strand, CCGTCCTAGCAAGAGGCTGCTACCGGAA, r′ strand, TCAACCACCGCTCGACTCAACTGCAGTC, and x strand, GACTGCAGTTGAGTCCTTGCTAGGACGG, to generate the three forms of junction S in which the methylphosphonate linkage (R_p, S_p, or racemic) is one nucleotide 5′ to the point of strand exchange. Radioactively 5′-^{32}P-labeled h or x strands were incorporated as appropriate. Junctions were purified by gel electrophoresis under nondenaturing conditions and electroelution.

Analysis of Cleavage Reaction Products by Mass Spectrometry. A version of junction 3 was constructed by hybridization of an h strand (the strand to be analyzed) of 28 nt and remaining strands each of 50 nt. The 112 μM junction was incubated with 23 μM endonuclease I (dimer) in 100 μL of 50 mM Tris-HCl (pH 7.5), 50 mM NaCl, 0.5 mM DTT, and 0.1 mg/mL BSA for 60 min at 20 °C. Cleavage was initiated by adding 10 mM $MgCl_2$ (final concentration) and the reaction terminated after 3 h by addition of 50 mM EDTA. The protein was digested with 0.5 mg/mL proteinase K for 30 min at 50 °C, and then the mixture was denatured at 95 °C and cooled on ice. The digest was diluted 10-fold with 0.1 M TEAA (pH 7.0), applied to a reversed-phase HPLC column (Waters μBondapak C18, 7.8 mm × 300 mm, 125 Å), and eluted with a gradient of 1−30% acetonitrile in 0.1 M TEAA at 2 mL/min over 50 min. Fractions were collected, twice dried under vacuum from deionized water, and finally resuspended in 5 μL of water. Samples of 1 μL (>200 μM) were mixed with an equal volume of 50 mg/mL ammonium citrate and 8 μL of 75 mg/mL 3-hydroxypicolinic acid matrix in 1:1 water/acetonitrile. Aliquots of 4 μL were analyzed using a Voyager DE-STR MALDI-TOF spectrometer (Applied Biosystems) in positive ion mode with an accelerator voltage of 20 kV.

Kinetic Analysis of Cleavage Rates. Cleavage rates were determined under single-turnover conditions. Endonuclease I (200 nM) was incubated with 40 nM junction radioactively 5′-^{32}P-labeled on one strand in 50 mM Tris-HCl (pH 7.5), 50 mM NaCl, and 100 μg/mL BSA (binding buffer) for 15 min at room temperature to allow the complex to form. The cleavage reaction was initiated by adding divalent metal ion solution to a final concentration of 10 mM, and the reaction was terminated at chosen time intervals by addition of formamide containing 120 mM EDTA, either using a QFM400 quench-flow mixer (Bio-Logic, Grenoble, France) or manually. After denaturation by heating to 95 °C for 5 min, substrate and product were separated by electrophoresis in 15% polyacrylamide gel containing 7 M urea at 80 W for 45 min. Dried gels were exposed to storage phosphor screens (BAS-IP MP 2040) and quantified using a BAS-1500

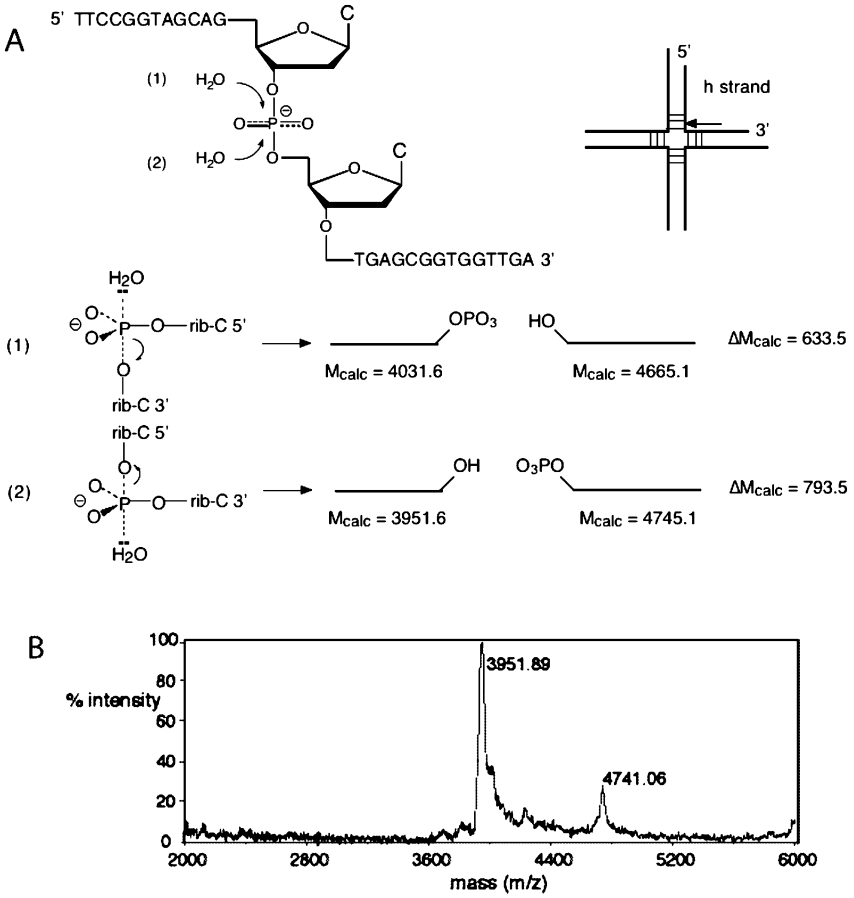

FIGURE 1: Analysis of the direction of attack by the water nucleophile in endonuclease I cleavage of a DNA junction. (A) The principle of the experiment. The top shows the sequence of the strand used, with the two possible directions of attack at the scissile phosphate indicated. Attack opposite the 5′ oxygen atom (1) leads to a calculated mass difference between the two products of 633.5 Da, while attack opposite the 3′ oxygen atom (2) leads to a mass difference of 793.5 Da. (B) MALDI-TOF mass spectrometric analysis of the products of endonuclease I cleavage of junction 3. The mass spectrum shows two clear peaks with masses of 3951.9 and 4741.1 Da. Following cleavage the DNA was desalted and fractionated by reversed-phase HPLC, and the fraction taken for mass spectrometry did not contain stoichiometrically equivalent quantities of the two product oligonucleotides.

phosphorimager (Fuji) and MacBAS v2.5 software. Reaction progress curves were fitted to an empirical model in which a fraction (*A*) of the complexes undergo a rapid cleavage reaction (rate k_{cl}), while the remaining species require a slower conversion (rate k_{con}) before cleaving at rate k_{cl}. This leads to the integrated rate equation:

$$F_{cleaved} = A(1 - (\exp(-k_{cl}t))) + (1 - A)(1 + (k_{cl}\exp(-k_{con}t) - k_{con}\exp(-k_{cl}t))/(k_{con} - k_{cl})) \quad (1)$$

For the reactions performed at different pH values, the buffers used were MES (pH 5.5−6.8), Bis-Tris (pH 5.8−6.3), HEPES (pH 6.8−8.1), Tris-HCl (pH 7.5−9.0), and CHES (pH 9.0−9.8), each at 50 mM.

RESULTS

Direction of Attack of the Water Nucleophile. In principle, hydrolysis of the phosphodiester bond could proceed by attack of a water molecule from a direction that is opposite either the 5′ or the 3′ oxygen atom (Figure 1A). These alternative mechanisms will have different outcomes, leading to the linkage of the scissile phosphate to the 5′ or 3′ oligonucleotide products, respectively. We have analyzed the products of the cleavage of the junction 3 h strand by T7 endonuclease I under multiple-turnover conditions, using MALDI-TOF mass spectrometry. The calculated molecular masses of the products according to the alternative mechanisms are shown in Figure 1A. Breakage of the P−O5′ bond leads to a difference in calculated mass of 633.5 Da between the two products, while breakage of the O3′−P should give a mass difference of 793.5 Da. The resulting mass spectrum has two clear peaks with masses of 3951.9 and 4741.1 Da, a difference of 789.2 Da (Figure 1B). These results clearly support the mechanism that leads to breakage of the bond to the 3′ oxygen atom, i.e., mechanism 2 in Figure 1A. This direction of nucleophilic attack is common to the restriction enzymes (*30*) and homing endonucleases such as I-*Cre*I (*39*).

Construction of a Permuted Junction Containing a Resolved Methylphosphonate Linkage. The next question we addressed concerned the different roles of the nonbridging oxygen atoms of the scissile phosphate in the cleavage reaction. This was explored by the substitution of these atoms by methyl groups. This has two potential effects. First, the resulting methylphosphonate group is electrically neutral. Second, the replacement of oxygen by methyl could interfere with interactions in which the oxygen would normally participate. We would expect that substitution of the *proR* and *proS* oxygen atoms would have different consequences, beyond that of charge neutralization.

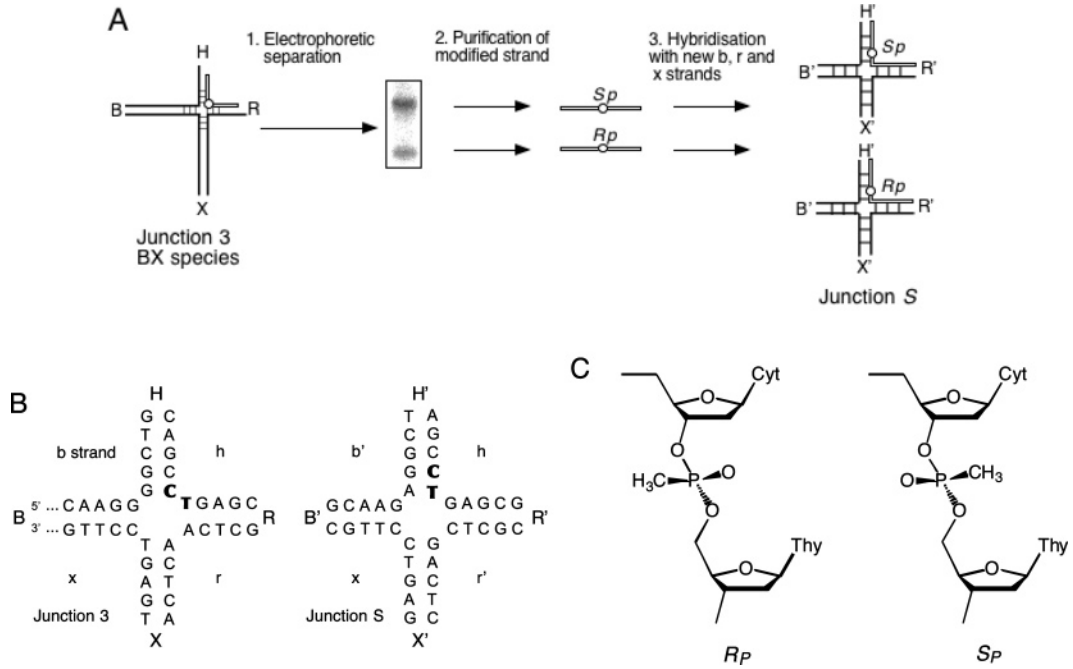

FIGURE 2: Principle of the construction of a junction containing a resolved methylphosphonate at the scissile phosphate linkage. (A) A form of junction 3 with long B and X arms and short H and R arms was constructed. It contains an h strand (shown in open type) of 28 nt with a central methylphosphonate group (indicated by the circle). Two forms of the junction were separated by gel electrophoresis in the presence of 200 μM Mg^{2+} ions, containing a methylphosphonate linkage of either R_p or S_p configuration. The gel shown is an example but not the actual one used for the strand separation. The modified h strands were purified by denaturing gel electrophoresis and separately hybridized with three new strands to generate junction S in which the modified phosphate was located one step 5′ to the point of strand exchange. (B) The central sequences of junctions 3 and S. The names of the corresponding arms and strands (except for strands h and x which are unchanged) of junction S are given primes to distinguish them from junction 3. The CmpT dinucleotide containing the methylphosphonate linkage is highlighted in bold type. (C) The stereochemistry of the CmpT linkage. The configuration of the methylphosphonate linkage in the R_p and S_p forms is shown.

Substitution of a nonbridging oxygen by methyl generates a stereogenic center, and for this study it was necessary to resolve the two diastereomers. We have recently shown that a junction containing a methylphosphonate group on the continuous strand (i.e., one of the two strands associated with a single axis that relates two stacked helices in the junction) can migrate as two quite separate and noninterconverting species in which the methylphosphonates have opposite chirality (*38*). This results from differential stabilization of the opposite stacking conformers by the two diastereomers, and this can be used to resolve relatively long DNA oligonucleotides containing a methylphosphonate linkage. However, this separation method requires that the methylphosphonate group be located at the center of the junction (i.e., potentially at the point of strand exchange), whereas the scissile phosphate is located one nucleotide to the 5′ of this position. It was therefore necessary to carry out the resolution using one junction [the well-studied junction 3 (*40*)] and then to use the modified h strand to construct a new junction with the methylphosphonate (as a CmpT dinucleotide) at the required position for cleavage (Figure 2). Thus the new junction S was constructed by hybridizing the modified strand h with three new strands such that the entire strand became translocated by one nucleotide in the 5′ direction thereby placing the CpT step 5′ to the point of strand exchange. Three forms of the junction were created in which the methylphosphonate had S_p (i.e., the *proR* oxygen was replaced by methyl) or R_p (*proS* oxygen was replaced by methyl) configuration or a racemic mixture of each.

Endonuclease I Cleavage of the Junction with the Translocated Linkage. Before analyzing the cleavage of the modified junction, it was necessary to characterize the cleavage of the new junction S by endonuclease I. For this purpose we constructed a form of this junction with helical arms of 13 or 15 bp, comprising DNA in which all phosphate linkages were unmodified, including that of the h strand. Four forms of the junction were prepared, individually radioactively 5′-^{32}P-labeled on a single strand. Cleavage reactions were initiated by addition of Mg^{2+} ions to a final concentration of 10 mM to the preformed enzyme−junction complex under single-turnover conditions in a quenched-flow mixer, and the reaction was terminated by chelation of metal ions with EDTA. The products of the cleavage reaction were separated by electrophoresis on a sequencing gel and quantified by exposure of the gel to storage phosphor screens and phosphorimaging. Cleavage was observed to be strongly biased, giving ~90% cleavage of the h and diametrically opposed x strand, indicating that the complex is heavily biased toward the conformer in which these strands are continuous strands (Figure 3). A good fit to the kinetic data was obtained using a model (eq 1) in which one fraction (70%) of the complexes underwent rapid cleavage, while the remaining fraction required a slower unknown conversion event before cleavage. This model gave rates of cleavage of 5.0 ± 0.7 s^{-1} for the h strand and 5.6 ± 0.5 s^{-1} for the opposing x strand, values that are comparable with those measured previously for cleavage of junction 3 (*41*). This junction was therefore suitable for studying the effect of methylphosphonate substitutions at the scissile phosphate linkage.

The Presence of Methylphosphonate 5′ to the Center of the Junction Does Not Perturb Endonuclease I Cleavage of

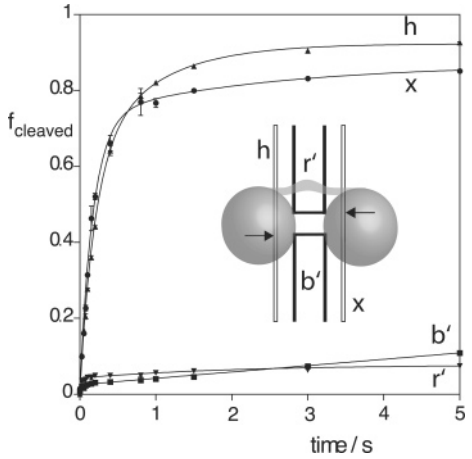

FIGURE 3: Kinetics of endonuclease I cleavage of the permuted junction S. Four versions of junction S comprising four arms of 13 or 15 bp were constructed in which one strand was radioactively 5′-^{32}P-labeled and the remaining strands were unlabeled. In separate experiments, these were incubated with endonuclease I under single-turnover conditions. The reactions were initiated by addition of Mg^{2+} ions to 10 mM in a quench-flow mixer, and the reactions were terminated by chelation with EDTA. The products were separated by polyacrylamide gel electrophoresis under denaturing conditions, and the extent of strand cleavage was estimated by phosphorimaging. Reaction progress (as fraction cleaved $f_{cleaved}$) is plotted as a function of time, fitted to the empirical rate equation (eq 1). Extents of cleavage of different strands are indicated by the following symbols: h, triangles; x, circles; b′, squares; r′, inverted triangles. The insert shows a scheme of the major conformer of the junction−enzyme complex, in which the h and x strands (shown by open lines) are continuous, while the b and r strands (black) are exchanging. Arrows denote the point of cleavage on the continuous strands.

the Diametrically Opposite Strand. The kinetics of cleavage by endonuclease I were then studied for the junction with methylphosphonate substitution at the scissile phosphate (i.e., 5′ to the center) of the h strand, in R_p or S_p configuration or as the racemic mixture of diastereomers. Before analyzing the cleavage of the modified phosphate, we studied the cleavage of the corresponding phosphate group on the diametrically opposed x strand (the dinucleotide TpC), using the same analysis as that for the unmodified junction above (Figure 4A). The strand was cleaved to ~80% for all three modified junctions, with rates in the range of 4.6−7.0 s^{-1}. Thus the extent and rates of cleavage are very similar to those for the unmodified junction, and we conclude that the formation of an active complex of endonuclease I and the junction is not compromised by the presence of the methylphosphonate linkage on the h strand. We could therefore proceed to a study of the cleavage at the modified phosphate itself.

Stereospecific Effects of Substitution of Nonbridging Oxygen Atoms by Methyl at the Scissile Phosphate. Endonuclease I cleavage of the h strand of junction S was analyzed under single-turnover conditions as above. The scissile phosphate group was replaced with methylphosphonate of R_p or S_p configuration or as the racemic mixture of diastereomers (Figure 4B). Cleavage rates were severely reduced in all three species. The junction containing the racemic mixture was cleaved at a rate of 1.6 (±0.1) × 10^{-2} s^{-1}, approximately 2 orders of magnitude lower than that measured for the unmodified junction. However, the effect is very stereospecific. Replacement of the *proS* oxygen by

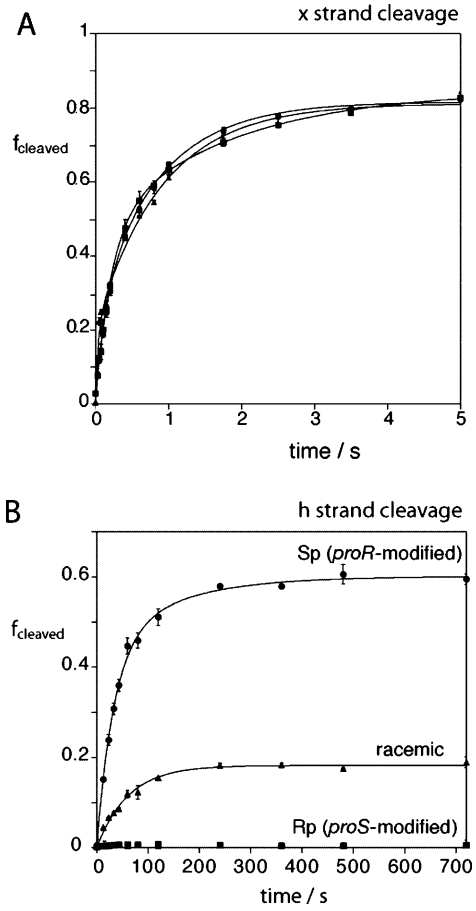

FIGURE 4: Kinetics of endonuclease I cleavage of junction S with stereospecific methylphosphonate substitution at the scissile phosphate linkage. (A) Cleavage of the x strand that is diametrically opposed to the strand with methylphosphonate substitution. Junctions were assembled containing radioactively 5′-^{32}P-label on the x strand, with methylphosphonate substitution on the h strand with R_p, S_p, or racemic configuration. (B) Cleavage of junction S at the methylphosphonate linkage of the h strand. In these experiments the modified strand (R_p, S_p, or racemic configuration) was radioactively 5′-^{32}P-labeled. In both experiments, endonuclease I cleavage was performed under single-turnover conditions, using a quench-flow mixer. The extent of reaction was quantified by electrophoretic separation of products and phosphorimage analysis. All of the data have been fitted to the empirical rate equation (eq 1). Symbols: R_p (squares), S_p (circles), or racemic (triangles).

methyl (R_p configuration) led to a more severe impairment of the cleavage reaction than the *proR* substitution (S_p configuration). Indeed, cleavage of the *proS*-modified junction was virtually undetectable, and no rate could be measured. By contrast, the junction in which the *proR* oxygen was replaced by methyl was cleaved at a rate of 2.2 (±0.06) × 10^{-2} s^{-1}, and the strand was ultimately cleaved to nearly 60%. The cleavage of the racemic mixture was approximately an average of the two diastereomers; we attribute the slightly lower extent of cleavage in the racemic mixture to a bias toward the R_p form during synthesis as revealed by HPLC analysis (data not shown). We conclude that replacement of the scissile phosphate by an electrically neutral methylphosphonate group leads to a marked loss in cleavage rate by endonuclease I but that the nonbridging oxygen atoms are far from equivalent. Evidently the *proS* oxygen atom plays a more significant role in the chemistry of cleavage than the *proR* oxygen.

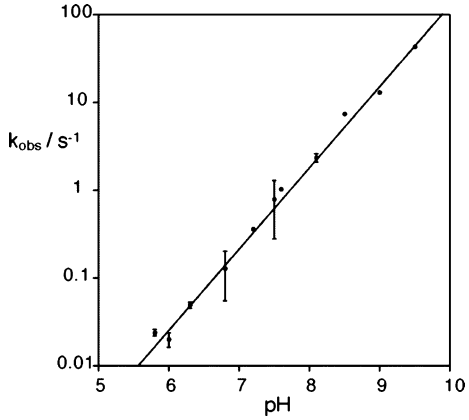

FIGURE 5: Dependence upon pH of the rate of cleavage of junction 3 by endonuclease I. The rate of hydrolysis of the h strand of junction 3 by endonuclease I was measured in triplicate as a function of buffer pH in the presence of 10 mM Mg^{2+} ions. The rate has been plotted on a logarithmic scale as a function of pH, and the data were fitted to eq 2 corresponding to *n* proton transfers required for formation of the active form of the enzyme. Error bars are standard errors.

pH Dependence of Phosphodiester Bond Hydrolysis by Endonuclease I. A water molecule is a relatively poor nucleophile, and we would expect it to require de-protonation by a general base to facilitate attack upon the phosphate group. Requirement of a proton transfer event prior to the transition state should result in a pH-dependent reaction, and we have therefore investigated the dependence of the cleavage rate on buffer pH. Junction 3 radioactively 5′-^{32}P-labeled on the x strand was incubated with endonuclease I under single-turnover conditions in the presence of 10 mM Mg^{2+} ions; preliminary experiments showed this to be a saturating concentration of the metal ions. Reactions were performed as a function of buffer pH over the range 5.8−9.8, each rate being measured in triplicate. Five different buffer systems (each 50 mM; see Materials and Methods) were used to cover this range; these included overlapping pH values to check for buffer dependence, although no scaling of data was in fact required. The observed rates of bond cleavage have been plotted as a function of pH in Figure 5. The logarithm of the rates depends linearly on pH over the full range. The data have been fitted to an equation corresponding to *n* proton transfers required for formation of the active form of the enzyme:

$$k_{obs} = k_{cat}/(1 + 10^{pK_A - npH}) \quad (2)$$

where k_{cat} is the cleavage rate of the deprotonated enzyme, pK_A is the acid dissociation constant of the group undergoing proton transfer, and *n* the number of protons transferred. An excellent fit ($R = 0.997$) was obtained with a value of $n = 0.9$, indicating the transfer of a single proton to form the active enzyme. Because the rate is log-linearly dependent on pH up to the highest value studied, a value of the pK_A of the titrating group could not be obtained. However, simulation of the data indicated that the p$K_A \geq 9$. We have performed analogous experiments in the presence of 10 mM Mn^{2+} ions. Similar results were obtained, with a log-linear dependence of rate over the range 5.8−9.5 and a gradient of 1.1 (Figure S1, Supporting Information).

Effect of Conservative Mutation of Active Site Acidic Side Chains. The above results are consistent with an in-line attack by a metal ion-coordinated hydroxyl ion. The two metal ions of the active site are principally bound by the carboxylate side chains of Asp 55 and Glu 65, and their positioning should be critical in providing the optimal geometry of attack. We have therefore explored the effect of the mutations of active site aspartate for glutamate and vice versa, i.e., E20D, D55E, and E65D. The results are presented in Figure 6, showing the cleavage products following a 60 min incubation of x strand 5′-^{32}P-labeled junction 3 with endonuclease I. Under these conditions, the wild-type enzyme generates 80% conversion to cleaved junction at 2 s^{-1} (*41*). However, no cleavage was obtained with the D55E and E65D mutants in the presence of Mg^{2+} ions, with limited cleavage by the E20D mutant. Evidently the repositioning of the carboxylate groups due to the addition or removal of a methylene linkage has a major effect on the activity of the enzyme. Limited activity was restored by performing the incubation in the presence of Mn^{2+} ions, particularly for the E65D mutant. Moreover, the pH dependence of the cleavage rate with endonuclease I E65D in Mn^{2+} ions was closely similar to that of the wild-type enzyme ($n = 0.9$; Figure S2, Supporting Information), suggesting that the mechanism remains unaltered. In common with the wild-type enzyme, none of the mutants was active in the presence of 10 mM Ca^{2+} ions.

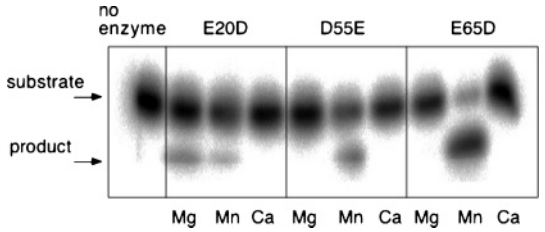

FIGURE 6: Activity of endonuclease I active site acidic mutants in the presence of different divalent metal ions. Junction 3 was incubated with endonuclease I E20D, D55E, or E65D for 60 min in the presence of 20 mM Mg^{2+}, Mn^{2+}, or Ca^{2+} ions. Substrate and products were separated by polyacrylamide gel electrophoresis and visualized by phosphorimaging.

DISCUSSION

In this study we have established that in the hydrolysis of the phosphodiester linkage by endonuclease I the water nucleophile attacks from the direction opposite to the 3′ oxygen atom and that the *proS* oxygen atom plays a particularly critical role. These observations provide some insight into the catalytic mechanism of the junction-resolving enzyme. The direction of attack is the same as that found in the restriction enzymes (*30*). We have modeled the structure of endonuclease I bound to a DNA junction (*41*), based in part on the close similarity between the active site to that of *Bgl*I (Figure 7). Cleavage of the two strands by endonuclease I is not simultaneous, and this aspect will probably require crystallographic investigation in due course (J. Hadden, S. E. V. Phillips, A.-C. Déclais, and D. M. J. Lilley, unpublished data), but the present model probably provides a good indication of the geometry of the active site immediately prior to cleavage. The identification of the direction of attack of the hydrolytic water molecule in the present study supports our previous contention that this is water molecule II coordinated to metal ion 1 that is bound in turn by the carboxylate groups of Asp 55 and Glu 65 and the main chain carbonyl of Thr 66 (*29*). This water molecule is aligned for

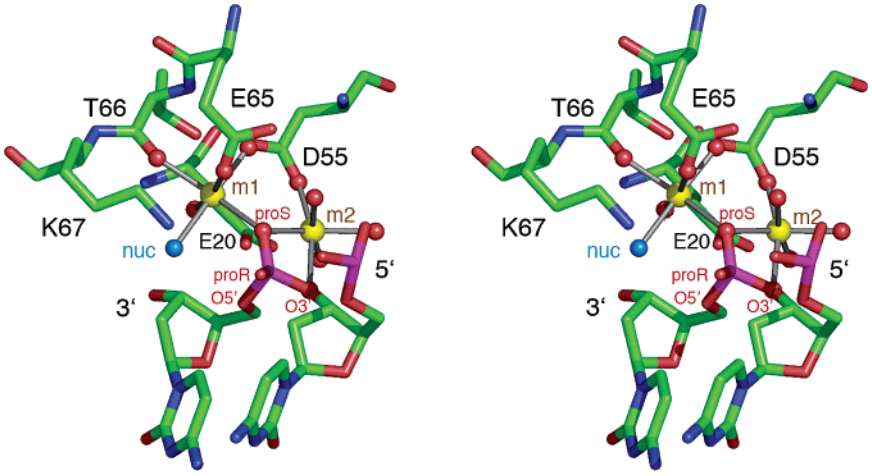

FIGURE 7: Parallel-eye stereoscopic view of a model of a dinucleotide bound to the active site endonuclease I, showing the two bound metal ions and associated water of hydration. In an earlier modeling exercise, a four-way junction was complexed with the crystal structure of endonuclease I and associated Mn^{2+} ions (*41*), guided in significant part by the structure of *Bgl*I complexed with DNA (*31*). The water molecules of hydration coordinating the two metal ions (m1 and m2) have been added to this view of the active site, using the positions of the water molecules bound to the Mn^{2+} ions as observed in the crystal structure of the free protein (*29*). The water molecule coordinated to m2 opposite to the D55 oxygen in the free protein has been replaced by the 3′ oxygen atom of the scissile phosphate. Note that the water molecule (nuc, highlighted in cyan) coordinated to metal ion 1 is well positioned for in-line attack on the scissile phosphorus opposite the 3′ oxygen leaving group. In this model, the *proS* oxygen atom is coordinated to both metal ions (replacing a water molecule that bridges the ions in the free protein), while the *proR* does not interact with either ion. The model is therefore very consistent with the observed order of effect *proS* > *proR* substitution, and the current results can be taken as further evidence for this model. The coordination of the two metal ions in this model is completely equivalent to that observed in the *Bgl*I−DNA complex (*31*).

in-line attack, opposite the 3′ oxygen atom of the scissile phosphate; breakage of the P−O3′ bond would lead to the observed products of hydrolysis.

Substitution of a nonbridging oxygen atom at the scissile phosphate leads to marked kinetic effects on hydrolysis at that site, with rates reduced by >100-fold. By comparison, there is no measurable effect at the corresponding phosphate on the other continuous strand, indicating that binding of the junction to the enzyme is unaffected. We conclude therefore that the effect of the substitution at the scissile phosphate is due to effects that occur in the transition state. Significantly, there is a pronounced difference in the magnitude of the effect between substitution of the individual prochiral oxygen atoms, with the larger effect arising from substitution of the *proS* oxygen atom such that cleavage was virtually undetectable for the R_p methylphosphonate. If we calculate a difference in free energy of activation from the kinetic data [$\Delta\Delta G^{\ddagger} = -RT \ln(k_{MeP}/k_P)$, where k_{MeP} and k_P are the rates for the substituted and unsubstituted species, R is the molar gas constant, and T is the absolute temperature], then $\Delta\Delta G^{\ddagger} = 12$ kJ mol^{-1} for the substitution of the *proR* oxygen but >28 kJ mol^{-1} for the *proS* oxygen atom.

The methylphosphonate substitution results are fully consistent with our model of the endonuclease I−DNA complex (*41*) (Figure 7), in which the *proS* oxygen atom is coordinated to both metal ions (Mn^{2+}−O distances of 2.5 and 2.6 Å), while the *proR* does not interact with either ion (Mn^{2+}−O distances ≥4.5 Å). The same features are observed in the cocrystal structure of *Bgl*I (*31*). Substitution of the *proR* oxygen atom should not interfere directly with ion binding, and thus the ∼100-fold reduction in cleavage rate is likely to represent the basic electrostatic effect arising from the removal of the negative charge from the phosphate group. By contrast, substitution of the *proS* oxygen by a methyl group will prevent direct contacts with both metal ions. While this does not appear to destabilize the ground state complex with the enzyme in a measurable way, the interaction is clearly important in the transition state, leading to an extremely low rate of hydrolysis.

The rate of the hydrolysis reaction exhibits a log-linear dependence on pH, with a gradient of 1, and corresponds to the titration of a group with a pK_A >9. The active site of the restriction enzyme *Eco*RV is another example of hydrolytic water in the coordination sphere of a metal ion bound to two carboxylate side chains (*42*, *43*). However, the pH dependence of *Eco*RV has been found to exhibit a gradient of 2 and a pK_A around neutrality (*44*), suggesting significant differences in mechanism, although an earlier study of the wild-type enzyme reported a gradient of unity (*45*). Nevertheless, a mutant of *Eco*RV was found to exhibit a pH dependence closely similar to that found for endonuclease I (*44*). The simple pH dependence of endonuclease I indicates that a single proton transfer is required to generate the active enzyme. The high pK_A is consistent with a hydroxide ion coordinated by metal ion 1 acting as the nucleophile in the hydrolysis reaction. Although other explanations remain possible, this interpretation is consistent with all of the available data and the mechanistic model (Figure 7) based upon the crystal structure of the enzyme and comparison with restriction enzymes such as *Bgl*I. The pK_A of the water should be reduced by virtue of its coordination to the magnesium ion, but it is nevertheless likely to be beyond the experimentally accessible range of pH.

Interactions between the scissile phosphate group and metal ions would be expected to be very sensitive to repositioning of the carboxylate groups in the active site. Activity of the mutants D55E and E65D was particularly affected, and no cleavage was detected with either mutant in the presence of Mg^{2+} ions. Since the charge and chemical nature of the side chains were unaltered by these conservative substitutions, the orientation and positioning of these residues

are clearly critical. Interestingly, some activity could be restored to these mutant enzymes by carrying out the reactions in the presence of Mn^{2+} ions. This effect was greatest for E65D. Nevertheless, the rate of cleavage of endonuclease I in Mn^{2+} ions was 250 times lower than the wild-type enzyme under the same conditions of pH and ionic strength; this corresponds to $\Delta\Delta G^{\ddagger} = 14$ kJ mol^{-1}. This rate reduction contrasts with the activity of E65Q endonuclease I, where the rate of cleavage in the presence of Mg^{2+} ions is only 100-fold reduced from the wild type (*36*). This again suggests that the position of the carboxylate groups, and hence that of the metal ions in the active site, is extremely important in order to achieve an efficient hydrolysis reaction.

In summary, our results are fully consistent with an in-line attack on the scissile phosphate of a metal-bound hydroxyl group opposite the 3′ oxygen atom. The *proS* oxygen of the DNA is probably coordinated to both metal ions in the transition state, and there is a key role for the carboxylate side chains in positioning the reactants. The emerging mechanism is closely similar to a number of restriction enzymes, supporting the view of an evolutionary relationship between these enzymes as previously suggested by phylogenetic comparisons (*15*).

ACKNOWLEDGMENT

We thank Drs. Jon Hadden and Alasdair Freeman for discussion, Douglas Lamont and Kenneth Beattie for assistance with mass spectrometry, and Dr. John Zhao for chemical synthesis of DNA.

SUPPORTING INFORMATION AVAILABLE

Figure S1 showing the pH dependence of the rate of cleavage of junction 3 by wild-type endonuclease I in the presence of Mn^{2+} ions and Figure S2 showing the pH dependence of the rate of cleavage of junction 3 by endonuclease I E65D in the presence of Mn^{2+} ions. This material is available free of charge via the Internet at http://pubs.acs.org.

REFERENCES

1. Lilley, D. M. J., and White, M. F. (2001) The junction-resolving enzymes, *Nat. Rev. Mol. Cell Biol. 2*, 433−443.
2. Fogg, J. M., Schofield, M. J., Déclais, A.-C., and Lilley, D. M. J. (2000) The yeast resolving enzyme CCE1 makes sequential cleavages in DNA junctions within the lifetime of the complex, *Biochemistry 39*, 4082−4089.
3. Fogg, J. M., and Lilley, D. M. J. (2001) Ensuring productive resolution by the junction-resolving enzyme RuvC: Large enhancement of second-strand cleavage rate, *Biochemistry 39*, 16125−16134.
4. Connolly, B., Parsons, C. A., Benson, F. E., Dunderdale, H. J., Sharples, G. J., Lloyd, R. G., and West, S. C. (1991) Resolution of Holliday junctions *in vitro* requires the *Escherichia coli ruvC* gene product, *Proc. Natl. Acad. Sci. U.S.A. 88*, 6063−6067.
5. Iwasaki, H., Takahagi, M., Shiba, T., Nakata, A., and Shinagawa, H. (1991) *Escherichia coli* RuvC protein is an endonuclease that resolves the Holliday structure, *EMBO J. 10*, 4381−4389.
6. Kemper, B., and Garabett, M. (1981) Studies on T4 head maturation. 1. Purification and characterisation of gene-49-controlled endonuclease, *Eur. J. Biochem. 115*, 123−131.
7. de Massey, B., Studier, F. W., Dorgai, L., Appelbaum, F., and Weisberg, R. A. (1984) Enzymes and the sites of genetic recombination: Studies with gene-3 endonuclease of phage T7 and with site-affinity mutants of phage *λ*, *Cold Spring Harbor Symp. Quant. Biol. 49*, 715−726.
8. Symington, L., and Kolodner, R. (1985) Partial purification of an endonuclease from *Saccharomyces cerevisiae* that cleaves Holliday junctions, *Proc. Natl. Acad. Sci. U.S.A. 82*, 7247−7251.
9. West, S. C., Parsons, C. A., and Picksley, S. M. (1987) Purification and properties of a nuclease from *Saccharomyces cerevisiae* that cleaves DNA at cruciform junctions, *J. Biol. Chem. 262*, 12752−12758.
10. White, M. F., and Lilley, D. M. J. (1996) The structure-selectivity and sequence-preference of the junction-resolving enzyme CCE1 of *Saccharomyces cerevisiae*, *J. Mol. Biol. 257*, 330−341.
11. Komori, K., Sakae, S., Shinagawa, H., Morikawa, K., and Ishino, Y. (1999) A Holliday junction resolvase from *Pyrococcus furiosus*: functional similarity to *Escherichia coli* RuvC provides evidence for conserved mechanism of homologous recombination in bacteria, eukarya, and archaea, *Proc. Natl. Acad. Sci. U.S.A. 96*, 8873−8878.
12. Kvaratskhelia, M., and White, M. F. (2000) Two Holliday junction resolving enzymes in *Sulfolobus solfataricus*, *J. Mol. Biol. 297*, 923−932.
13. Liu, Y., Masson, J. Y., Shah, R., O'Regan, P., and West, S. C. (2004) RAD51C is required for Holliday junction processing in mammalian cells, *Science 303*, 243−246.
14. Garcia, A. D., Aravind, L., Koonin, E., and Moss, B. (2000) Bacterial-type DNA Holliday junction resolvases in eukaryotic viruses, *Proc. Natl. Acad. Sci. U.S.A. 97*, 8926−8931.
15. Lilley, D. M. J., and White, M. F. (2000) Resolving the relationships of resolving enzymes, *Proc. Natl. Acad. Sci. U.S.A. 97*, 9351−9353.
16. Makarova, K. S., Aravind, L., and Koonin, E. V. (2000) Holliday junction resolvases and related nucleases: identification of new families, phyletic distribution and evolutionary trajectories, *Nucleic Acids Res. 28*, 3417−3432.
17. Ariyoshi, M., Vassylyev, D. G., Iwasaki, H., Nakamura, H., Shinagawa, H., and Morikawa, K. (1994) Atomic structure of the RuvC resolvase: A Holliday junction-specific endonuclease from *E. coli*, *Cell 78*, 1063−1072.
18. Raaijmakers, H., Vix, O., Toro, I., Golz, S., Kemper, B., and Suck, D. (1999) X-ray structure of T4 endonuclease VII: a DNA junction resolvase with a novel fold and unusual domain-swapped dimer architecture, *EMBO J. 18*, 1447−1458.
19. Hadden, J. M., Convery, M. A., Déclais, A.-C., Lilley, D. M. J., and Phillips, S. E. V. (2001) Crystal structure of the Holliday junction-resolving enzyme T7 endonuclease I at 2.1 Å resolution, *Nat. Struct. Biol. 8*, 62−67.
20. Bond, C. S., Kvaratskhelia, M., Richard, D., White, M. F., and Hunter, W. N. (2001) Structure of Hjc, a Holliday junction resolvase, from *Sulfolobus solfataricus*, *Proc. Natl. Acad. Sci. U.S.A. 98*, 5509−5514.
21. Ceschini, S., Keeley, A., McAlister, M. S. B., Oram, M., Phelan, J., Pearl, L. H., Tsaneva, I. R., and Barrett, T. E. (2001) Crystal structure of the fission yeast mitochondrial Holliday junction resolvase Ydc2, *EMBO J. 20*, 6601−6611.
22. Nishino, T., Komori, K., Tsuchiya, D., Ishino, Y., and Morikawa, K. (2001) Crystal structure of the archaeal Holliday junction resolvase Hjc and implications for DNA recognition, *Structure 9*, 197−204.
23. Studier, F. W. (1969) The genetics and physiology of bacteriophage T7, *Virology 39*, 562−574.
24. Center, M. S., and Richardson, C. C. (1970) An endonuclease induced after infection of *Escherichia coli* with bacteriophage T7. I. Purification and properties of the enzyme, *J. Biol. Chem. 245*, 6285−6291.
25. Sadowski, P. D. (1971) Bacteriophage T7 endonuclease. I. Properties of the enzyme purified from T7 phage-infected *Escherichia coli* B, *J. Biol. Chem. 246*, 209−216.
26. Kerr, C., and Sadowski, P. D. (1975) The involvement of genes 3, 4, 5 and 6 in genetic recombination in bacteriophage T7, *Virology 65*, 281−285.
27. Powling, A., and Knippers, R. (1976) Recombination of bacteriophage T7 in vivo, *Mol. Gen. Genet. 149*, 63−71.
28. Tsujimoto, Y., and Ogawa, H. (1978) Intermediates in genetic recombination of bacteriophage T7 DNA. Biological activity and the roles of gene 3 and gene 5, *J. Mol. Biol. 125*, 255−273.
29. Hadden, J. M., Déclais, A.-C., Phillips, S. E. V., and Lilley, D. M. J. (2002) Metal ions bound at the active site of the junction-resolving enzyme T7 endonuclease I, *EMBO J. 21*, 3505−3515.
30. Pingoud, A., and Jeltsch, A. (2001) Structure and function of type II restriction endonucleases, *Nucleic Acids Res. 29*, 3705−3727.

31. Newman, M., Lunnen, K., Wilson, G., Greci, J., Schildkraut, I., and Phillips, S. E. V. (1998) Crystal structure of restriction endonuclease *Bgl*I bound to its interrupted DNA recognition sequence, *EMBO J. 17*, 5466−5476.
32. Kovall, R. A., and Matthews, B. W. (1998) Structural, functional, and evolutionary relationships between lambda-exonuclease and the type II restriction endonucleases, *Proc. Natl. Acad. Sci. U.S.A. 95*, 7893−7897.
33. Ban, C., and Yang, W. (1998) Structural basis for MutH activation in *E. coli* mismatch repair and relationship of MutH to restriction endonucleases, *EMBO J. 17*, 1526−1534.
34. Hickman, A. B., Li, Y., Mathew, S. V., May, E. W., Craig, N. L., and Dyda, F. (2000) Unexpected structural diversity in DNA recombination: the restriction endonuclease connection, *Mol. Cell 5*, 1025−1034.
35. Freeman, A. D., Déclais, A.-C., and Lilley, D. M. J. (2003) Metal ion binding in the active site of the junction-resolving enzyme T7 endonuclease I in the presence and absence of DNA, *J. Mol. Biol. 333*, 59−73.
36. Déclais, A.-C., Hadden, J. M., Phillips, S. E. V., and Lilley, D. M. J. (2001) The active site of the junction-resolving enzyme T7 endonuclease I, *J. Mol. Biol. 307*, 1145−1158.
37. Beaucage, S. L., and Caruthers, M. H. (1981) Deoxynucleoside phosphoramidites—a new class of key intermediates for deoxypolynucleotide synthesis, *Tetrahedron Lett. 22*, 1859−1862.
38. Liu, J., Déclais, A.-C., McKinney, S. A., Ha, T., Norman, D. G., and Lilley, D. M. J. (2005) Stereospecific effects determine the structure of a four-way DNA junction, *Chem. Biol. 12*, 217−228.
39. Chevalier, B. S., Monnat, R. J., Jr., and Stoddard, B. L. (2001) The homing endonuclease I-CreI uses three metals, one of which is shared between the two active sites, *Nat. Struct. Biol. 8*, 312−316.
40. Duckett, D. R., Murchie, A. I. H., Diekmann, S., von Kitzing, E., Kemper, B., and Lilley, D. M. J. (1988) The structure of the Holliday junction and its resolution, *Cell 55*, 79−89.
41. Déclais, A.-C., Fogg, J. M., Freeman, A., Coste, F., Hadden, J. M., Phillips, S. E. V., and Lilley, D. M. J. (2003) The complex between a four-way DNA junction and T7 endonuclease I, *EMBO J. 22*, 1398−1409.
42. Winkler, F. K., Banner, D. W., Oefner, C., Tsernoglou, D., Brown, R. S., Heathman, S. P., Bryan, R. K., Martin, P. D., Petratos, K., and Wilson, K. S. (1993) The crystal structure of *Eco*RV endonuclease and of its complexes with cognate and noncognate DNA fragments, *EMBO J. 12*, 1781−1795.
43. Kostrewa, D., and Winkler, F. K. (1995) Mg^{2+} binding to the active site of *Eco*RV endonuclease: A crystallographic study of complexes with substrate and product DNA at 2 Å resolution, *Biochemistry 34*, 683−696.
44. Stanford, N. P., Halford, S. E., and Baldwin, G. S. (1999) DNA cleavage by the *Eco*RV restriction endonuclease: pH dependence and proton transfers in catalysis, *J. Mol. Biol. 288*, 105−116.
45. Sam, M. D., and Perona, J. J. (1999) Catalytic roles of divalent metal ions in phosphoryl transfer by *Eco*RV endonuclease, *Biochemistry 38*, 6576−6586.

BI0523254